Building and Environment 305 (2026) 115149

Contents lists available at ScienceDirect

Building and Environment

journal homepage: www.elsevier.com/locate/buildenv

Creating thermal refuges with low-energy cooling: effectiveness of evaporative coolers

Roberto Rugani [a,b,*,1], Maíra André [a,c,d,1], Marco Picco [e], Giacomo Salvadori [b], Stefano Schiavon [a,f,g], Roberto Lamberts [d], Hui Zhang [a]

[a] Center for the Build Environment, University of California, Berkeley, USA
[b] Department of Energy, Systems, Territory and Constructions Engineering (DESTEC), University of Pisa, Pisa, Italy
[c] IEQ Lab, School of Architecture, Design and Planning, The University of Sydney, Australia
[d] Laboratory of Energy Efficiency in Buildings, Federal University of Santa Catarina, Brazil
[e] School of Engineering and Computing, University of Lancashire, Preston, United Kingdom
[f] Department of Architecture, College of Environmental Design, University of California, Berkeley, USA
[g] Department of Civil and Environmental Engineering, College of Engineering, University of California, Berkeley, USA

ARTICLE INFO

Keywords:
Evaporative cooling
Thermal refuge
Low-energy cooling
PCS
PECS
Thermal comfort

ABSTRACT

Heatwaves increasingly endanger public health, underscoring the urgent need for low-energy cooling strategies suitable for emergency use. Among them, evaporative cooling (EC) systems represent a promising solution to create temporary thermal refuge areas with minimal energy and infrastructure requirements, especially under hot and dry conditions. However, experimental evidence on their real cooling potential, particularly under different ventilation and boundary conditions, remains limited. This study investigates the thermal performance of two EC systems, a whole-room unit and a personal-scale device, through laboratory tests in a controlled climate chamber (5 × 5 × 2.53 m) set at 32 °C. We assessed: (i) indoor air temperature and humidity offsets, (ii) spatial airflow and turbulence distributions, and (iii) cooling effects (CE) measured using a thermal manikin. We found that the whole-room EC reduced air temperature by up to 2.8 K and increased relative humidity from 15–20% up to 52%, while producing an average CE of 3 K on the manikin and over 5 K in upper body regions. When combined with a personal EC, the CE rose to 6 K, despite limited additional air temperature reduction. Spatial mapping revealed heterogeneous airflow and turbulence, which enhanced convective heat transfer. Energy demand was small (220 W and 10 W for the whole-room and personal ECs, respectively), while water consumption averaged 2.6 L/h (0.034 L/h·m^3). These findings show that evaporative cooling can provide rapid, effective thermal relief with low energy use, offering a scalable solution for protecting vulnerable populations during extreme heat events.

1. Introduction

Global climate change is expected to increase the duration, intensity, and frequency of heatwaves [1]. Although definitions vary across the literature [2], heatwaves generally refer to periods of unusually hot and dry weather relative to historical norms. The World Meteorological Organization (WMO) and World Health Organization (WHO) further characterize heatwaves as phenomena with a “discernible impact on human and natural systems” [3]. The associated health risks depend on a complex interplay of physiological, demographic, social, economic, and medical factors, and are particularly high for vulnerable populations such as children, elders, and individuals with chronic conditions, while also strongly affecting outdoor workers. Heat-related illnesses include heat exhaustion, heat stroke, acute kidney injury, and the worsening of cardiovascular and respiratory diseases [3–5].

In response to the escalating health threats posed by extreme heat, many cities have begun developing public infrastructure intended to serve as climate refuges [6,7]. These “climate shelters” offer temporary protection from extreme temperatures and often involve the repurposing of existing facilities such as libraries, civic centres, schools, or green spaces [8]. However, such shelters are often inequitably distributed, difficult to access for a significant portion of the at-risk population [9]. Furthermore, the brief exposure to cooling provided by these spaces may

* Corresponding author at: Center for the Build Environment, University of California, Berkeley, USA.
E-mail address: roberto.rugani@ing.unipi.it (R. Rugani).
[1] These authors contributed equally to the paper.

https://doi.org/10.1016/j.buildenv.2026.115149
Received 23 March 2026; Received in revised form 17 August 2026; Accepted 18 August 2026
Available online 19 August 2026
0360-1323/

Nomenclature

Acronyms

ACH	Air Changes per Hour (h^{-1})
CFD	Computational Fluid Dynamics
CE	Cooling Effect
DEC	Direct Evaporative Cooling
EC	Evaporative Cooler
EHT	Equivalent Homogeneous Temperature
HVAC	Heating, Ventilation, and Air Conditioning
IEC	Indirect Evaporative Cooling
OA	Outside Air
RH	Relative Humidity

Symbols

A	Body segment surface area [m^2]
h_c	Convective heat transfer coefficient [$W/m^2 \cdot K$]
I_{clo}	Clothing insulation effect [clo]
L	Characteristic length [m]
Q	Heat loss [W/m^2]
Re	Reynolds number [-]
SD	Standard deviation of air velocity [m/s]
T_{air}	Air dry bulb temperature [°C]
T_{sk}	Skin temperature [°C]
Tu	Turbulence Intensity [%]
U	Mean air velocity [m/s]
ρ	Air density [kg/m^3]
η	Dynamic viscosity of air [$N \cdot s/m^2$]

not be effective in limiting heat strain during a prolonged heatwave [10].

While climate shelters provide refuge at the community level, residential buffer zones are also proposed as a strategy for handling climate variability. Climate refuges in residential buildings are areas or rooms designed for climate adaptation, where localized microclimates allow occupants to remain safe during heatwaves [11,12]. Despite the important role of passive strategies in creating such microclimates [11], air Conditioning (AC) remains the most widespread solution for mitigating indoor heat exposure. Although effective in cooling occupants, AC requires large amounts of energy, increasing pressure on electricity grids and raising critical social issues related to access to cooling technologies [13]. AC global penetration is strongly income-dependent, being accessible primarily to high-income populations in many countries and reinforcing global inequalities in cooling access [14]. While approximately 90% of the U.S. population owns an AC unit, regions with much higher cooling demand, such as South-Central Asia and Africa, account for only 1–2% of U.S. AC stock [15]. With rising temperatures and more frequent heatwaves, the need for cooling is no longer just a matter of comfort – it is a matter of survivability [16]. Urgent, sustainable strategies are required to safeguard the most vulnerable [17].

Moreover, intense use of AC increases pressure on the electricity grid. During a heatwave in 2025, peak electricity demand increased by 25% in France, where AC ownership is low, whereas in New York it increased by up to 90%, as the ownership is very high [18]. Such increased demand can cause power shortages and blackouts, jeopardizing essential services. Therefore, using AC on peak hot days can be unreliable because of its effect on energy sources.

The high energy peaks also increase greenhouse gas emissions and heat island effects [19,20]. Compressor-based AC use is responsible for 65% of global hydrofluorocarbon emissions and is predicted to increase Earth's mean surface temperature [21].

Electric fans offer a low-energy cooling strategy by enhancing convective and evaporative heat loss through increased air movement across the skin [22]. They are low-cost equipment and consume as little as a few watts, about 3% of the energy required by conventional compressor-based AC systems, while also avoiding the negative environmental impacts associated with refrigerant gases [23]. Fans can be used alone as an alternative to AC or combined with AC, reducing compressor workload and overall energy consumption [23–29].

Despite the advantages of fan cooling, health authorities suggest that they should not be used when the ambient temperature exceeds skin temperature [30]. The threshold is set at 90°F (~32 °C) by the US Centre for Disease Control (CDC) [31] to 40 °C by WHO [5]. Some researchers claim there is limited empirical validation for the WHO limit [32] while others argue that there is enough validation [33].

Fan effectiveness depends not only on ambient temperature but also on humidity and the individual's sweat capacity. Under many warm and humid conditions, air movement increases the efficiency of sweat evaporation, making fans beneficial even when air temperature exceeds skin temperature [34,35]. Human subject tests of temperature thresholds have shown fans to be beneficial for young adults at 42 °C and 48% RH [36] and 40 °C 50% RH [35]. Fan use was not beneficial at 42 °C in humid conditions (>65%) for older adults aged 60–80 years, due to reduced sweating response [37]. Using a biophysical model, Morris et al. [38] examined the thresholds for healthy young adults, healthy older adults (assuming age-related sweat reduction of 25%), and older adults taking anticholinergic medication (an additional 25% sweat reduction). The authors proposed simplified thresholds for fan use regardless of humidity levels: 39 °C for healthy young adults, 38 °C for healthy older adults, and 37 °C for older adults taking anticholinergic medication. Tartarini et al. [39] used the human thermoregulatory model developed by Gagge et al. [40] to estimate heat losses and physiological variables as a function of environmental and personal factors. Depending on air speed, metabolic activity, and clothing insulation, the operative temperature threshold up to which healthy adults can use fans to reduce heat stress reaches up to 43.5 °C. Recent human subject experiments confirmed that, in healthy adults, fans can be safely used in environments at up to 43 °C with relative humidity as low as 25% [33]. However, under extremely hot and dry conditions, often observed during heatwaves, fans may be ineffective or detrimental, increasing convective heat gain when ambient temperature exceeds skin temperature. These findings suggest that the updated WHO guidance may still be conservative, although further research is needed to assess fan safety in older adults and other heat-vulnerable populations [33].

To address the limitations of fans in hot and dry environments, evaporative cooling can be used to lower the air temperature into a range where fan use becomes physiologically beneficial [41–45]. Evaporative coolers (EC) operate by exposing moving air to liquid water, triggering a phase change from liquid to vapor that is an endothermic process. To do that, a fan is combined with a wet porous material, called substrate or pad, through which air circulates, enabling heat exchange between the air and water [46–48]. The resulting evaporation process cools recirculated air back to space at a lower temperature and higher relative humidity. However, the cooling performance of EC systems strongly depends on boundary conditions, particularly ambient temperature and relative humidity [49–51]. The benefit of EC over air-conditioning systems is its reduced energy demand, comparable to fans but with a higher cooling effect [52–61]. The cooling effect is the reduction in uniform air temperature that would produce the same thermal sensation or heat loss as the condition with the assessed equipment [62,63]. In addition to energy, EC has an environmental benefit of reducing the use of refrigerants and associated greenhouse gas emissions [42].

Fans and evaporative coolers have been recently recognized as important strategies to mitigate AC use in present and future climate change scenarios [15]. Nevertheless, while the effects of electric fans on thermal comfort in indoor spaces have been widely studied, most publications on EC address its use as a part of an air-conditioning system [59,64–66] or focus on indirect evaporative cooling (IEC) systems. Several comprehensive review studies have analyzed their working principles, configurations, and performance enhancement strategies, including both experimental and modelling approaches [67–74]. These works highlight the significant potential of IEC systems as energy-efficient alternatives to conventional air-conditioning, as well as their wide applicability across diverse climatic conditions and system configurations. However, compared to the extensive body of work on indirect systems, experimental data and investigation of direct evaporative cooling (DEC), particularly portable equipment, are addressed in very few publications, indicating an important research gap.

Besides their thermal performance, portability, cost, maintenance, and energy demand are important factors considering the use of evaporative coolers in refugee areas during extreme conditions. Portable equipment is usually more affordable than ducted and wall-mounted equipment, allowing this strategy to be extended to a broader population and deployed only during periods of extreme heat demand. Additionally, EC can consume 62–74% less energy than air conditioning when used to cool a room [60], while personal evaporative coolers operate at very low power (around 10 W) and can still provide significant cooling by acting closer to the user [75].

Among the available publications, Camargo et al. [65] tested the temperature reduction generated by an evaporative cooler, comparing indoor, outdoor and the outlet temperatures of the cooler. The equipment was used during summer in a warm city in Brazil with outdoor temperatures from 25–32 °C. The maximum temperature difference between the outside and the outlet temperature was 7.4 K, and the maximum difference between indoor and outdoor temperatures was 3.5 K. Rugani et al. [60] found that the temperature and relative humidity offset generated by an evaporative cooler depends on outdoor conditions. The authors simulated an EC in EnergyPlus during heatwaves in 4 cities with different climates. Results showed broader temperature drops and moderate relative humidity increases for drier-warmer climates. The maximum offset was 12 K and 65% of relative humidity in a room at 42 °C and 40% outdoor conditions. Under 34 °C and 27% outdoor conditions, the offset was reduced to a 3.5 K temperature drop and a 35% increase in relative humidity.

Sudprasert [59] tested the thermal perception impact of a portable EC in an office-like space during a hot-dry season in Thailand, with ambient air temperatures at 29.0–33.1 °C and relative humidity lower than 50%. The equipment produced an average thermal sensation of −0.6 on the 7-point thermal sensation scale, between neutral and slightly cool. Under the same conditions, a fan produced an average thermal sensation of 0 (neutral), indicating the evaporative cooler delivered a greater cooling effect. However, at high-speed operation, the fan resulted in higher overall satisfaction. Fifty-four percent of participants preferred thermal conditions not to change when using the fan, compared with 40% when using the evaporative cooler.

André et al. [76] found a preference for a small evaporative cooler over different desk fans. The thermal conditions of this experiment were less warm and more humid (average 28 °C, 70%) than those typically observed during heatwaves. Although half of the participants would prefer to buy the personal EC instead of the other 3 fans tested, they considered its cost too high when disclosed at the end of the experiment. André et al. [75] tested the effect of this EC against the best-rated fan and another, more affordable EC. The affordable EC was almost 4 times cheaper than the one tested by human participants. The tests with a thermal manikin indicated the affordable EC to achieve a higher cooling effect, of 2.9 K against 2.2 K of the other EC and 1.4 K by the fan. This result showed that an affordable personal evaporative cooler can produce significantly higher heat loss in the human body than a desk fan.

Despite the potential reported in the literature, the number of available studies remains limited. Previous investigations have largely relied on simplified simulation approaches, such as adapted EnergyPlus modules, that lack the necessary inputs to accurately represent water consumption, energy use, and the magnitude of temperature reductions produced in the occupied environment [60]. Moreover, the spatial distribution of the cooling effect, which is critical for informing realistic user guidance, is not captured by such modelling frameworks. In this context, experimental measurements using real devices offer significant advantages, enabling the assessment of their non-uniform impact on the indoor environment and occupants, as well as the interaction between room-level and personal-level equipment.

This work aims to verify the effectiveness of using portable direct evaporative coolers to create indoor thermal refuge areas, considering the combination of a system designed to affect the space (whole-room) and another designed to affect a person directly (local). We assessed effectiveness by quantifying the ability of evaporative coolers to: (i) reduce indoor air temperature while increasing relative humidity, and (ii) increase occupants' heat loss during warm conditions. Additionally, we mapped the spatial distribution of these effects in a room to recommend optimal positioning for heatwave events.

2. Method

The method involves four steps. To address the first objective, we monitored the temperature and relative humidity offset produced by the whole-room evaporative cooler (EC) in a controlled environment (1). After reaching a stable thermal condition, we mapped the indoor environmental parameters to understand their spatial distribution (2). To meet the second objective, we estimated the cooling effect of the whole-room (3) and local (4) evaporative coolers with a thermal manikin. These steps are further explained in the following order: Section 2.1 Whole-room EC temperature and relative humidity offset; Section 2.2 Whole-room EC manikin test; Section 2.3 Whole-room EC spatial mapping; Section 2.4 Local EC manikin test and spatial mapping.

In this study, the cooling effect is defined as the equivalent reduction in uniform air temperature under still air conditions that would produce the same heat loss as that induced by the tested cooling device [62,63].

We conducted all experiments at the University of California climate chamber in Berkeley. The chamber is 5.5 × 5.5 × 2.5 m, including two insulated internal walls and two insulated external walls with triple-glazing windows. The chamber's HVAC system controls both the room air temperature and the temperature in the external wall and window cavity [77]. Table 1 presents the characteristics of whole-room evaporative cooler, and a local personal evaporative cooler selected in a previous experiment [75].

2.1. Whole-room temperature and RH offset

To understand how much a whole-room evaporative cooler could offset the room temperature and increase relative humidity, we ran the whole-room evaporative cooler (EC) in the climate chamber at 32 °C with three HVAC configurations to mimic real-life conditions:

- HVAC On - In this scenario, the whole-room EC ran while the HVAC operated continuously without outdoor air (recirculation mode). This scenario represents the expected behavior of a non-insulated building with closed windows during a heat wave. The poor envelope allows external heat flux, which is mimicked by the HVAC injecting warm air and heating the air cavity between the internal and external chamber walls, while humidity exchange remains limited.
- HVAC Off - In this scenario, after the chamber reached a stable 32 °C, we turned the HVAC off and turned the whole-room EC on. Outdoor air was not used at any time. This scenario represents the behavior of a well-insulated building, where heat flux and humidity exchange to outdoors is minimized.

Table 1
Evaporative coolers characteristics.

Equipment	Whole-room evaporative cooler	Local evaporative cooler
Pictures	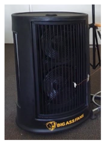	
Dimensions (l x w x h in m)	0.45 (diameter) x 0.85	0.20 × 0.20 × 0.25
Power (W)	220 (low)	10.6 (high) - 4.6 (low)
Water storage capacity (L)	30	0.5
Number of fans	2	1
Air speed at outlet (m/s)	3.8 (low)	1.9 (high) - 1.4 (low)
Substrate material	 Cardboard honeycomb	 Plastic structure with vertical felt slats

- HVAC On with Outdoor Air (OA) - In this scenario, the whole-room EC ran while HVAC operated continuously with outdoor air, with heat recovery and heaters maintaining a stable air temperature. This scenario replicates a naturally ventilated room with windows open, where heat flux and humidity exchange between indoors and outdoors are maintained.

The HVAC system was operated exclusively in heating mode in all scenarios to reproduce heatwave boundary conditions.

We monitored the chamber dry-bulb temperature and relative humidity with a HOBO® temperature/RH data logger (Model UX100-003 Onset, USA) every 1 min, which has a range of ± 0.21 °C from 0° to 50 °C, and accuracy of± 3.5% from 25 to 85% at 1 m height. We also measured the EC outlet temperature and relative humidity at 60 cm height, every 5 min with the high-precision digital thermometer (Model DP9601, Omega, USA), which has an accuracy of ± 0.01 °C and a humidity meter probe (Model HM 34, VAISALA, Finland), which has an accuracy of± 2% from 0 to 90%.

The whole-room EC includes fans and a pump that circulates water that drips over the cardboard honeycomb pad (see Table 1). Before starting the measurements, we filled the tanks with water, started to run the water pump and waited a few minutes to allow the pad to be soaked. We then turned on the fans at a minimum speed (3.8 m/s at 25 cm from the outlet). In each scenario, we monitored the thermal conditions for 50 min, after which temperature and humidity readings reached a steady state.

2.2. Whole-room EC manikin test

We estimated the whole-room cooling effect by placing a thermal manikin (Model 3.x, PT Teknik, Denmark) during the three scenarios described in Section 2.1.

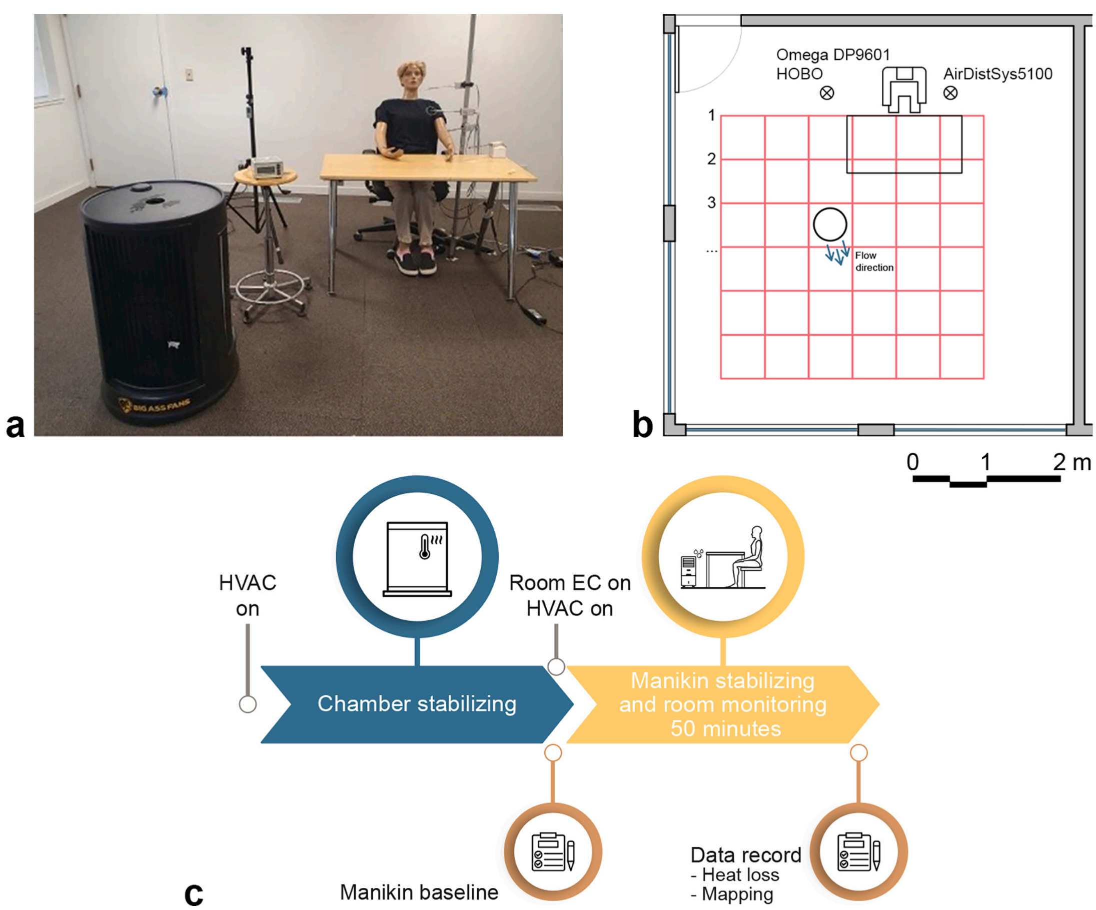

Fig. 1. Whole-room experiment setting: (a) picture of the chamber setting with manikin and EC position, (b) climate chamber floor with grid representing mapping measurement spots (49 points as points overlapping the table were not measured), circle indicating the whole-room EC position and outlet direction by arrows and a crossed circle indicating placement of fixed sensors, (c) experiment procedure indicating order of systems activation and recording moments.

Fig. 1a and b show the layout of the chamber during the tests (photo and floor plan). The manikin was in a sitting position in an office chair behind a desk, dressed in summer clothing, 0.5 clo. The evaporative cooler (black cylinder in a) was facing the wall, so the strong air flow would not hit the manikin directly but would circulate and humidify the air of the room (see Fig. 1b for outlet direction represented by arrows).

Fig. 1c indicates the test procedure, which started after thermal conditions in the chamber stabilized. The thermal manikin software recorded skin temperature and dry heat loss at 16 body segments (without the effect of perspiration) at 30-second intervals. For the cooling effect calculation, we used the average values from the final 5 min of each test condition, when the manikin responses (skin temperature and heat loss) were stable. This procedure was repeated twice: before activating the EC (baseline) and at the end of the test with the EC on. Section 2.5 explains how we used this data, as well as the room temperature, to calculate the cooling effect.

2.3. Whole-room EC spatial mapping of temperature and airflow

To better understand the cooling effect of the whole-room evaporative cooler, we mapped the distribution of air flow, air temperature, and turbulence. Fig. 1b shows the position of the points used in the mapping, defined by a regular grid of 7 × 7 squares (60 cm x 60 cm) covering the entire chamber. At each intersection, we placed a pole with five hotwire anemometers data loggers (Model AirDistSys5100, Sensor-Electronic, Poland), which have an accuracy of ± 0.2 °C, ± 0.02 m/s, at five heights: 10 cm, 60 cm, 110 cm, 170 m and 210 m. We recorded the variables for 5 s and averaged the results. We performed the mapping for the scenario of HVAC On with whole-room EC On, to guarantee prolonged stable conditions. We refilled the EC water whenever necessary to keep it running with constant performance.

2.4. Local EC manikin test

We evaluated the local evaporative cooler (local EC) using the same manikin-based procedure adopted for the whole-room EC. Fig. 2 illustrates the test layout and procedure. As shown in Fig. 2a, the local EC was positioned 50 cm to the left of the manikin, with the slats angled to direct airflow toward the chest, replicating the user-preferred configuration identified in a previous study with human subjects [76]. Fig. 2b shows the placement of four hot-wire anemometer data loggers (AirDistSys5100, Sensor-Electronic, Poland) used to measure air temperature and velocity in the region between the device and the manikin.

Fig. 2c summarizes the procedure adopted to assess the local EC cooling effect. We collected the baseline measurements under stable indoor conditions with the HVAC on (recirculation mode, no outdoor air) and the whole-room EC operating. After switching on the local EC and allowing thermal conditions to stabilize (about 50 min), we recorded skin temperature and dry heat loss from the manikin at the end of each test.

We tested the local EC with a dry pad, working as a fan, and with a wet pad to produce evaporative cooling effect. We also tested the equipment at two speed levels, the maximum (high) and minimum (low) (see Table 1 for details). Associating pad status (wet/dry) and air speed level (low/high), we performed four tests: dry-low, dry-high, wet-low and wet-high. Section 2.5 presents the calculation of the cooling effect we applied to each condition using the last 5-min average measurements.

2.5. Data processing

We tabulated the loggers' data and manikin results in Excel or CSV format. We performed data processing in R and RStudio version 2025.09 with the following packages: *tidyverse* [78], *metrics* [78], *ggpubr* [78], *extrafonts* [78], *scales* [78], *pacman* [79], *here* [80], *lubridate* [81].

We calculated Cooling Effect (CE in K) using equations 1 – 3, in which "j" represents one of the 16 manikin body parts. The overall CE is calculated with the sum of all body parts, each weighted by its corresponding surface area. Eq. (1) calculates the real insulation effect of the clothes on the manikin ($I_{clo,j}$ in clo) calculated with baseline conditions. T_{air} (°C) is the air temperature, $T_{sk,j,0}$ (°C) the skin temperature, and $Q_{j,0}$ (W/m^2) the heat loss [82]. Eq. (2) calculates the Equivalent

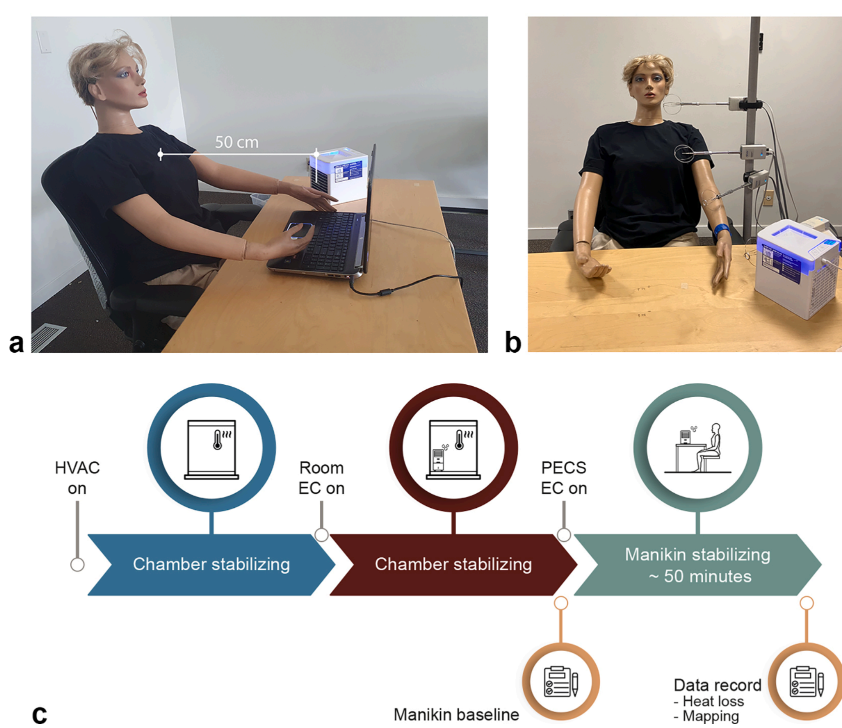

Fig. 2. Chamber setting with manikin to assess personal EC, (a) EC positioned 50 cm from manikin chest, (b) anemometers placed in 4 points to map local EC airflow distribution, (c) experiment procedures indicating order of systems activation and recording moments.

Homogeneous Temperature (EHT_j in K) when ECs were on. Eq. (2) includes the manikin's skin temperature ($T_{sk,j}$), heat loss (Q_j), body part surface area (A_j in m^2) and clothing insulation from Eq. (1) ($I_{clo,j}$). Finally, Eq. (3) calculates the cooling effect (CE_j in K) by comparing the EHT with the baseline air temperature (T_{air} in °C) [82].

$$I_{clo,j} = \left(T_{sk,j,0} - T_{air}\right) / \left(Q_{j,0}\cdot 0.155\right) \text{ [clo]} \quad (1)$$

$$EHT_j = T_{sk,j} - \frac{Q_j}{A_j}\cdot I_{clo,j}\cdot 0.155 \text{ [K]} \quad (2)$$

$$CE_j = T_{air} - EHT_j \text{ [K]} \quad (3)$$

Based on the test conditions and probes' accuracy, we estimated the uncertainties of the CE, following the methods applied in [83]. Those uncertainties are expressed by error bars of 95% confidence intervals in the analysis.

The graphical representation of the spatial mapping involved interpolating the collected data. Golden Software Surfer® (version 25.2) allows this interpolation, producing the isoline images.

3. Results

3.1. Whole-room EC temperature and RH offset

Fig. 3 shows the chamber and EC outlet air temperature and relative humidity (RH) trends for all tested scenarios.

We conducted all tests with the evaporative cooler operating at its lowest power setting (220 W). Fig. 3a shows that the HVAC on and HVAC on OA scenarios achieve similar temperature offsets between t(0) and t(50), of approximately 2.0 K. The HVAC off scenario (dashed magenta line) shows the highest temperature reduction of around 2.8 K. All scenarios show a strong initial temperature drop during the first 10 min, followed by a stabilization after approximately 30–40 min. However, the HVAC off scenario exhibits a slightly different rate of change. In both HVAC on scenarios, the temperature dropped about 1.2 K after 15 min, 1.6 K after 30 min, and reached roughly 2.0 K by 50 min. In contrast, the HVAC off scenario shows a greater offset, of 1.8 K after 15 min, 2.4 K after 30 min, and a final reduction of 2.8 K. The omitted values in the first 5 min are below the sensor range. Despite those differences, all scenarios reached a similar final temperature at t(50), of 29.5 ± 0.2 °C.

Fig. 3b shows that active HVAC operation helped moderate humidity levels while the evaporative cooler ran. Relative humidity stabilized at 39 and 44%, whereas the HVAC off scenario reached 52%. Similar to the temperature trend, relative humidity changed rapidly during the first 10 min, increasing by 14–18% after 15 min. From 15 to 30 min, RH increased more slowly (3–10%) and stabilized by t(50), at approximately 46 ± 7%. A major concern when using the Evaporative Cooler is the potential rise in indoor humidity; however, the maximum observed RH of 52% remains comparable to standard cooling design conditions [84].

Fig. 3c and d show the air temperature and relative humidity offsets at the EC outlet. The outlet temperature changes shown in Fig. 3c were smaller than the room-level temperature reductions shown in Fig. 3a. In the HVAC off scenario, the outlet temperature increased by nearly 3 K over 50 min, whereas it rose by only 0.5 K in the HVAC on scenario and remained nearly constant in the HVAC on OA scenario. These patterns reflect how the surrounding humidity conditions influenced the amount

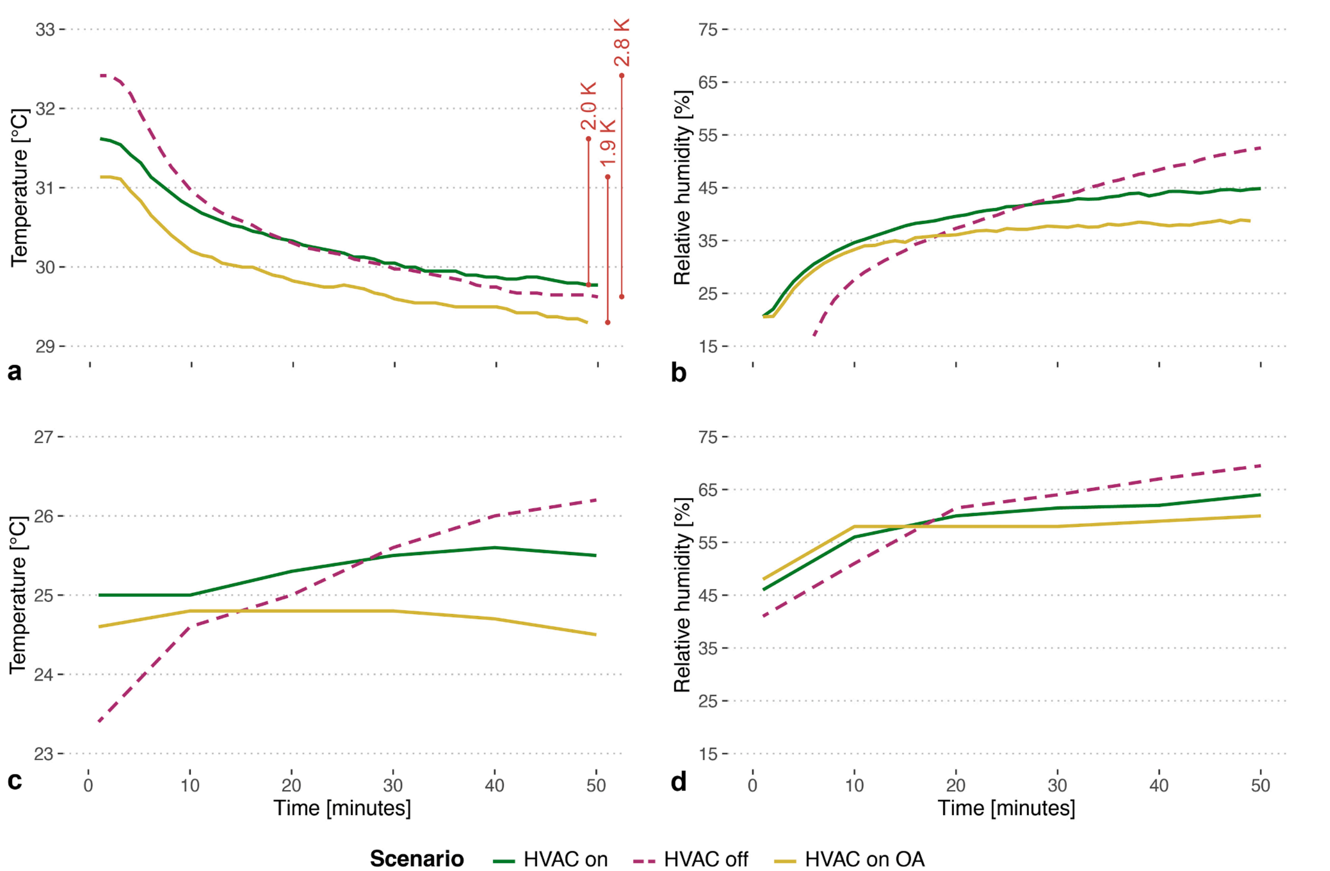

Fig. 3. Trends of (a) room air temperature, (b) room relative humidity, (c) EC outlet air temperature, and (d) EC outlet relative humidity through time. Red lines on the right side of figure (a) indicate the maximum delta temperature per scenario. Dashed lines indicate tests in which the HVAC system was turned off at minute 0, while solid lines refer to tests where the HVAC remained in operation (on) throughout the experiment. HVAC on OA includes outdoor air, while HVAC on scenario outdoor air was off, and the system only recirculated indoor air.

of evaporative cooling that could occur. Nevertheless, the EC maintained cooling potential, as outlet temperatures (∼25–26 °C) consistently remained below room air temperatures (∼30 °C). A similar pattern appears in Fig. 3d After 50 min, the outlet RH remained between 60–70% while room RH stayed around 45%, indicating a sustained cooling effect.

3.2. Whole-room EC cooling effect

The thermal manikin experiment quantifies the cooling effect (CE) of the whole-room evaporative cooler for each body segment by measuring the manikin's dry heat loss, expressed in Equivalent Homogeneous Temperature (EHT). The CE, in kelvin [K], indicates how much the system can shift perceived temperature toward neutrality. We performed the manikin test under the 3 HVAC scenarios. Fig. 4a presents the mean CE values with error bars derived from experimental uncertainty, and Fig. 4b is a visual representation of the mean CE per body part. The orange point in Fig. 4a presents the overall CE ("All"), a surface-area-weighted average calculated automatically by the manikin software. The overall mean CE of 3 ± 1.5 K indicates a substantial improvement in expected perceived temperature.

Fig. 4 shows a clearly greater effect on the upper body, from the hands and chest to the head. Most of the upper–body parts, except the back, show a CE of around 5 K, while most of the lower-body parts show an average CE of about 2.5 K. Nevertheless, higher cooling effects also exhibit higher uncertainty, approximately ∼3 K for the upper-body and ∼1 K for the lower-body. The left forearm (L. Forearm) reached the highest mean CE at 5.6 ± 3 K. A slight left-right imbalance appears in the results, with the left side (L.) generally showing stronger effects than the right (R.). This asymmetry, together with the lower effects on the lower body, may result from the airflow pattern generated by the EC as well as the shielding from the table and chair. For example, the back shows an average CE about 1.5 K lower than other upper-body parts because the chair block directs airflow from the EC. To better understand the cause of these differences, the next section examines spatial airflow, temperature, and turbulence mapping.

3.3. Whole-room EC mapping

This section presents the measured temperature distribution, air velocity, and turbulence maps when the whole-room evaporative cooler was operating with HVAC on. Fig. 5a-c show the horizontal temperature distribution at three heights. The lowest temperatures appear Fig. 5directly in front of the EC. At floor level (10 cm), the temperature reaches 29.5 °C, while at 60 cm and 110 cm the temperature is more than one degree higher (30.8 °C and 30.6 °C, respectively). The temperature pattern in Fig. 5a-c also show that the area near the manikin (behind the table) maintains similar temperatures at all heights, around 31.5 °C.

Fig. 5 d-f show the air speed distribution produced by the whole-room EC. Air speed is highest at floor level (10 cm), and the flow is deflected upward, resulting in higher air speed at 110 cm than at 60 cm in front of the device. Near the manikin, however, all three heights show the same air speed (0.2 m/s), indicating a uniform air distribution in that region.

Fig. 5 g-i present the turbulence distribution across the room, calculated as the standard deviation (SD) of the air speed measurements divided by the mean. Lower air speed typically produces higher turbulence because of the smaller mean value. However, the highest turbulence zones in Fig. 5 g-i do not correspond to the lowest air speed in Fig. 5 d-f. Instead, greater turbulence appears between the air jet direction and the adjacent wall, where the air flow bounces after hitting the wall in front of the EC. This pattern is especially evident at 10 and 110 cm heights (Fig. 5g and i). At 60 cm height, the highest turbulence occurs close to the front wall, along the path of the air jet. Overall, Fig. 5 g-i show that turbulence around the manikin is not the lowest in the room and exhibits more variation than the central region, reaching approximately 33%.

The sections in Fig. 6 AA'-III further illustrate how the airflow hits the floor and generates higher turbulence near the manikin from bottom to top. The plan-view navigator at the bottom of the figure shows the section positions. Fig. 6 BB'-III shows that the EC outlet is 2 °C cooler than the room temperature (32 °C), whereas Fig. 6 AA'-I shows that this temperature offset does not reach the manikin; the area closest to the manikin is only 0.2 °C cooler than the room.

3.4. Local EC cooling effect

In addition to the whole-room evaporative cooler, we added a personal evaporative cooler to evaluate how low-power equipment directed to the user could provide additional cooling under the same conditions. Fig. 7 shows the results from the manikin experiment. The results are presented for two air speeds (high and low) and two pad conditions: a wet pad with a full tank, and a dry pad with an empty tank. Values are shown for all body parts as well as for the "upper front" group (head, chest, arms and hands). The cooling effect (CE) on the upper-front areas exceeds the whole body ("All") body CE by approximately 1.5–2.2 K.

When the local EC operates with a dry pad, it functions as a fan, generating only convective heat loss on the manikin. In this dry-pad mode, Fig. 7 shows that the whole-body CE reaches 2 K at low air speed and 2.3 K at high air speed. For the upper-front parts, the CE reaches 3.5 K and 4.2 K at low and high air speeds, respectively. Adding water (wet-pad mode) increases both the overall and upper-front cooling under both air speeds. The evaporative effect from the wet pad

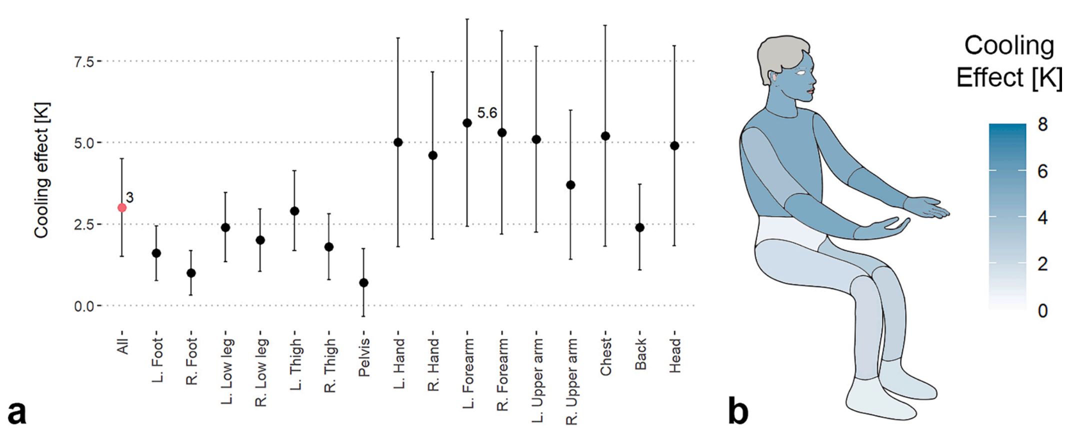

Fig. 4. Cooling effect of whole-room EC per body part (a) mean values and 95% confidence intervals (error and uncertainty); (b) Graphical representation of mean on the anatomical regions of the manikin (results are shown in color gradient). In the graph, L. stands for left and R. stands for right.

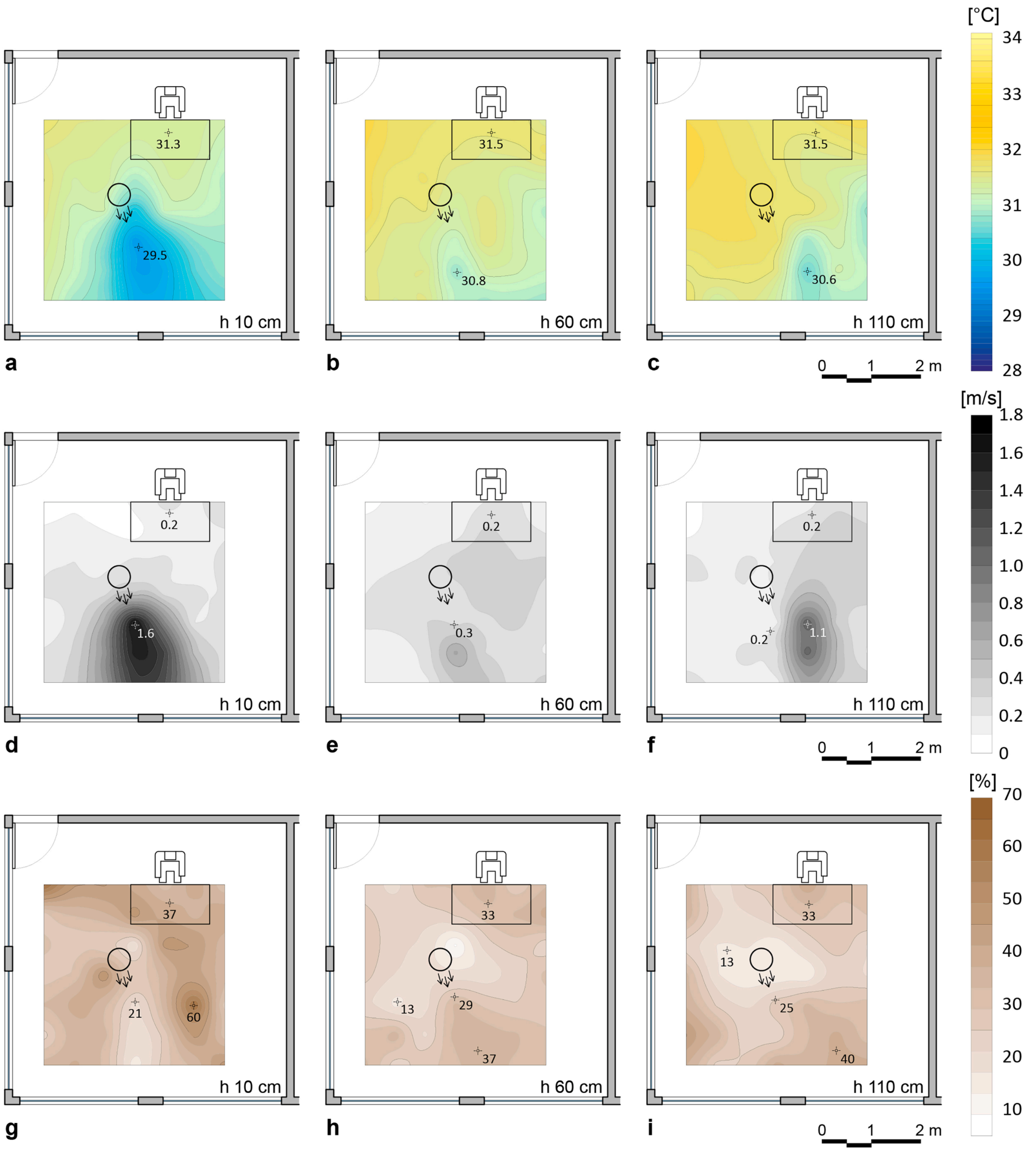

Fig. 5. Horizontal distribution of air temperature (a-b-c), air speed (d-e-f) and temperature (g-h-i) in the chamber with the whole-room EC active (represented by a circle). The arrows in front of the EC indicate the outlet location. Floor plan representation of three height measurements, at (a-d-g) 10 cm, (b-e-h) 60 cm and (c-f-i) 110 cm from the ground. Results are shown in a color gradient, with key values numerically indicated. The manikin's position and table are also represented in the floor plan.

increases CE by 0.2–0.8 K for the whole body and 0.4–1.1 K for the upper-front parts. Increasing air speed leads to greater enhancement than adding water; however, under high air speed, the wet pad still provides a substantial additional benefit, increasing the CE by more than 33%.

The local evaporative cooler adds 3.1 K of whole-body cooling and 5.3 K of upper-body cooling, even when the whole-room evaporative cooler is already operating. Such gains are remarkable given its minimal power demand of just 10 W.

Fig. 8 shows that the cooling effect is not evenly distributed across the body. As expected, the local EC cools only the upper body and particularly the left side of the manikin, which is positioned closer to the device outlet. Under the high-speed wet-pad condition, the upper arm experiences the highest CE (7.9 K), followed by the left forearm (7.0 K) and chest (6.7 K). Conversely, the right hand shows the lowest upper-body CE under dry-pad conditions (0.8–1.0 K). The head experiences

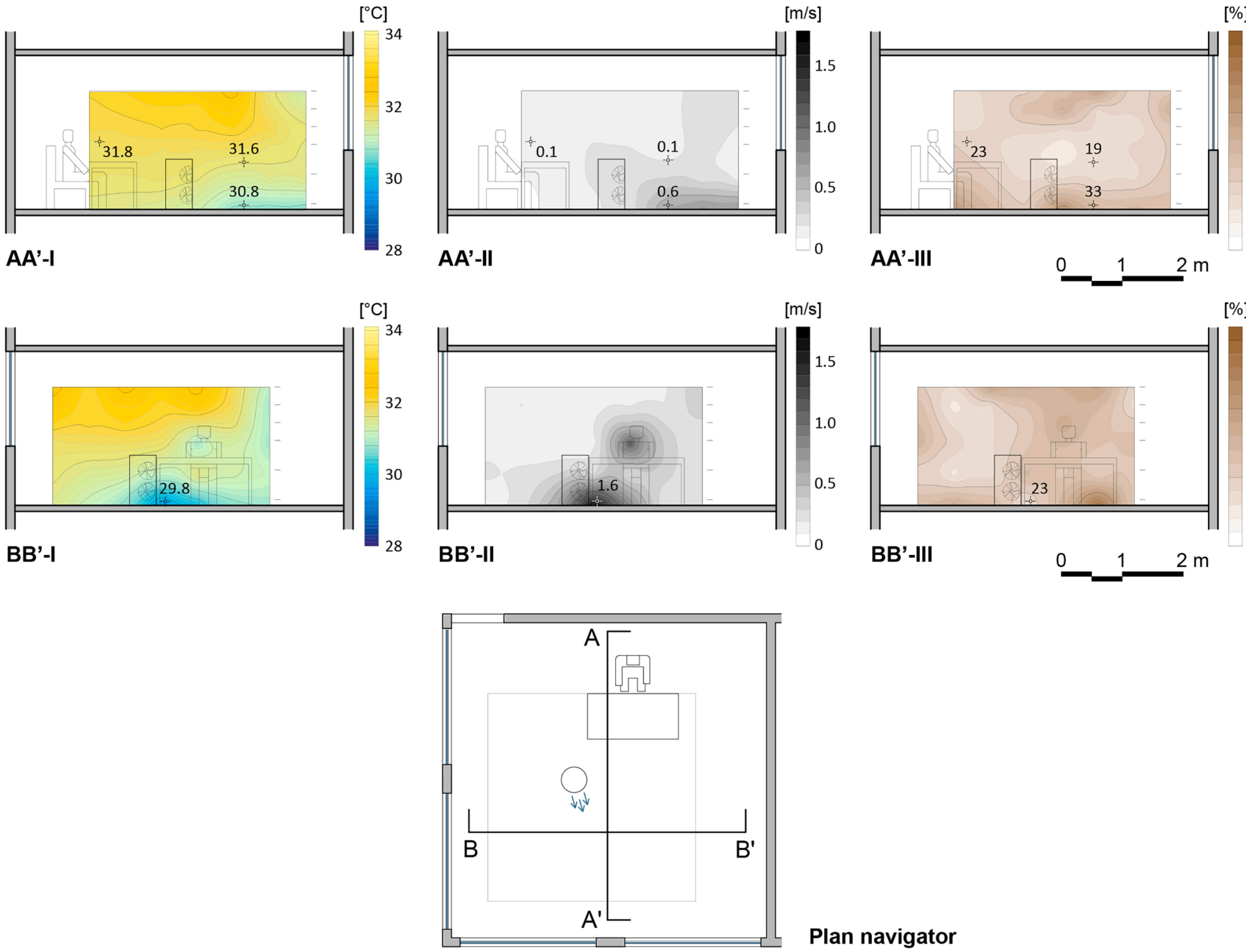

Fig. 6. Vertical distribution in the chamber when whole-room EC is active, A indicates section AA' and B for section BB', positioned as indicated in the plan navigator. And the other terms are the variable, I) temperature, II) air speed, and III) turbulence intensity. Results are shown in color gradient, and important points are numerically indicated. The EC is represented by a rectangle with fans positioned according to the outlet direction.

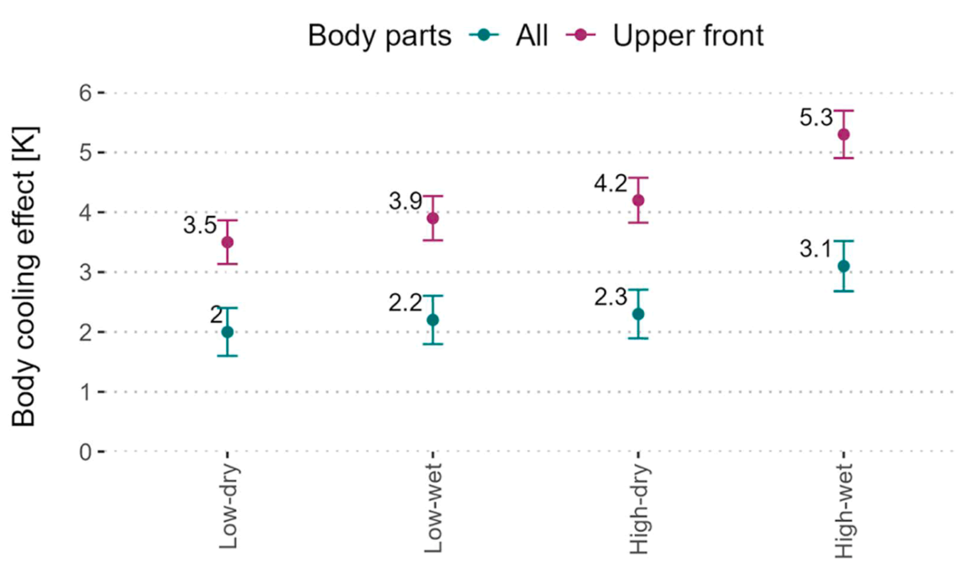

Fig. 7. Cooling effect of local evaporative cooler over all body parts (green) and upper front body parts (magenta). Labels represent air speed (low/high) and pad condition (without water = dry, with water = wet). Error bars represent 95% confidence intervals considering errors and uncertainty.

moderate CE (4.8–6.5 K), consistent with its partial exposure to the airflow.

Overall, wet-pad operation enhances the cooling performance across most body parts compared to dry-pad operation, and higher air speed

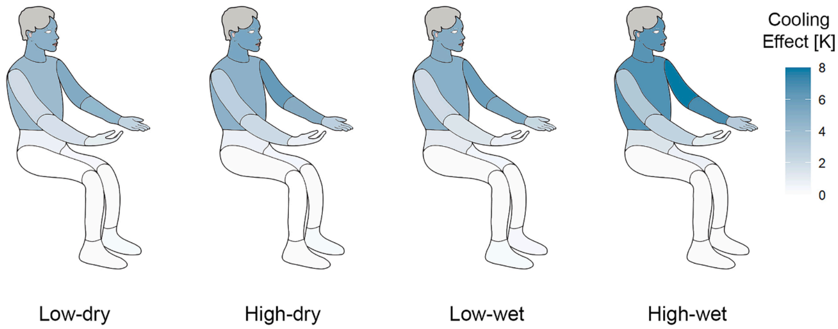

Fig. 8. Cooling effect of local evaporative cooler in association with the whole room evaporative system per body part presented by color gradient. Labels represent air speed (low/high) and pad conditions (without water = dry, with water = wet).

amplifies this effect while extending the cooled area. This combination of high airflow and evaporative effect promotes greater heat loss, particularly on the side facing the device outlet, although asymmetry remains due to the left-side placement of the device. To further interpret these differences, Appendix A provides a spatial mapping of air temperature and velocity between the local EC and the manikin.

4. Discussions

4.1. Thermal effect of evaporative coolers

The current experimental results demonstrate that evaporative coolers can potentially improve indoor thermal comfort by increasing occupants' heat loss in hot and dry conditions. Although the room temperature decrease is relatively limited (approximately 2–3 K), the cooling effect achieved by associating the whole-room and personal EC is substantial, up to 6 K. The whole-room EC alone provides only half of this effect, although been the only responsible for shifting the room temperature, underscoring the importance of evaluating cooling systems using metrics beyond room air temperature.

The combined cooling effect of both ECs indicates a theoretical perceived temperature shift from 32 to 26 °C, which indicates a great physiological effect towards thermal neutrality. This result highlights the substantial increase in body heat loss generated by the combined evaporative cooling strategies. Nevertheless, human subject experiments are necessary to assess the corresponding impacts on thermal sensation and comfort. These results should therefore be interpreted within the experimental limitations discussed in this and the following sections.

For instance, because the thermal manikin used in the experiments does not sweat, our results represent a conservative estimate; additional latent heat loss from human perspiration would boost the cooling effect. Evaporative coolers also raise indoor humidity, potentially reducing perspiration heat loss. Thus, overall physiological benefit reflects the balance between increased air movement, lower air temperature, and higher relative humidity [36]. Tartarini et al. [39], for example, estimated that sweating increased by 1.6 °C the limits of temperature in which a fan would not cause heat strains (under 60% RH). Compared to the dry-pad fan mode, the personal evaporative cooler increases its impact by 1–1.5 K when the pad is wet.

Additionally, previous research shows that targeting the torso and head provides greater thermal sensation reduction due to the high density of thermal receptors in these areas [85]. Both whole-room and personal EC deliver stronger effects on the chest and head, with a cooling effect around 5 K, which likely amplifies thermal sensation offset. Prior studies have shown that cooling specific body regions can disproportionately influence overall thermal comfort [86]. The combined experimental evidence therefore reinforces the potential of whole-room and personal evaporative cooling, especially when targeted toward upper-body regions, to provide meaningful thermal relief under warm indoor conditions.

4.2. Turbulence

The relatively high turbulence intensity may enhance the convective heat transfer coefficient (h_c), thereby increasing the local cooling capacity and amplifying the perceived cooling effect on the manikin. This mechanism may help explain why the evaporative cooler produced a strong cooling effect, measured by the thermal manikin, despite only modest reductions in air temperature.

The result section reported a turbulence intensity of about 33% near the manikin, while the mean air velocity ranged around 0.2 m/s, and the local temperature reduction of 0.5–0.7 K. Although these environmental changes are moderate, previous studies have shown that turbulent fluctuations can intermittently increase local velocity gradients, disrupt the thermal boundary layer at the body surface, and enhance convective heat exchange. As a result, convective heat losses may be underestimated if turbulence is neglected [87]. Nevertheless, most evidence in the literature derives from experiments conducted at air speeds much higher than those typical of indoor environments and those measured in the present study.

In a wind tunnel study with velocities above 4 m/s, Hunt et al. [88] reported significant turbulence effects on human performance and perception. Mayer [89,90] evaluated lower-range air speeds (< 0.5 m/s) and found that increasing turbulence intensity modestly enhanced convective heat loss. Similarly, Yu et al. [87], observed that increasing turbulence intensity from 15 to 30% at 0.9 m/s raised h_c by roughly 1.5 W/m^2K, still far above the velocities measured in our experiment. Xu et al. [91] investigated non-uniform airflow patterns typically of fans and showed that turbulence intensity can significantly influence h_c; however, the effect remained limited below 1.5 m/s.

Overall, these studies suggest that turbulence intensity can enhance convective heat transfer under certain airflow conditions. However, because most of the evidence comes from experiments with higher air velocities, the role of turbulence under the present low-speed conditions (~ 0.2 m/s) should be interpreted cautiously.

To provide a simplified numerical check, we calculated turbulence intensity (Tu) from the standard deviation and mean air velocity, using Eq. (4). Near the manikin (mean velocity U = 0.1 m/s, standard deviation SD = 0.03 m/s), the turbulence intensity effectively equals 30%.

$$Tu = \frac{SD}{U} = 30\% \tag{4}$$

Using these airflow conditions (U = 0.1 m/s, T = 32 °C, characteristic length L = 0.2 m, corresponding to an average manikin part diameter, such as the head), we calculated the Reynolds number with Eq. (5).

$$Re = \frac{(\rho \cdot U \cdot L)}{\eta} = \frac{(1.15 \cdot 0.1 \cdot 0.2)}{1.90 \cdot 10^{-5}} \approx 1210 \tag{5}$$

Where:

$\rho = 1.2\ kg/m^3$

$\eta = 1.9 \cdot 10^{-5}\ N \cdot s/m^2$

This Reynolds number characterizes a laminar regime (Re < 2300), indicating that the airflow around the manikin cannot be classified as fully turbulent. Nevertheless, the relatively high turbulence intensity measured near the manikin suggests that even small velocity fluctuations may enhance convective heat transfer. Recent CFD studies on evaporative cooling systems have also shown that including turbulence modelling can improve the prediction of EC performance even under relatively low Reynolds number conditions, due to local mixing phenomena and transient flow structures [92]. However, given the limited evidence available for turbulence-driven heat exchange at such low air speeds, further research is required to clarify the role of micro-scale airflow variability in shaping convective cooling and perceived thermal relief from evaporative systems.

4.3. Cooling refuge areas during heat waves

Results indicate that evaporative coolers can potentially create refuge areas during heat waves by significantly increasing occupants' heat loss during hot and dry conditions. In ecology, thermal refuges are areas that prevent organisms from being exposed to extreme conditions [93], which were achieved in the test conditions with the association of the ECs.

Unlike other species, humans can deliberately create thermally safe spaces. Architectural design can passively generate protective microclimates using strategies such as thermal mass, shading, vegetation, or increased natural ventilation. Nevertheless, when passive measures are insufficient or unavailable, active systems become essential. However, these systems must operate with low energy demand to prevent stress on the grid and remain affordable to run. Additionally, they must respond quickly because they are needed during emergency conditions.

Fig. 3 shows that the whole-room evaporative cooler produces the greatest air temperature reduction in the first 10 min of operation, lowering temperature by approximately 1 K. This rapid response can alleviate thermal strain, while sustained use can progressively increase heat loss from the body. Spatial mapping (see Fig. 5) revealed substantial variations in temperature and airflow distribution within the tested indoor space. Directly in front of the equipment, a buffer zone forms where air speed reaches 1.1–1.6 m/s and temperature is reduced by 1–1.5 K. This buffer zone could function as a refuge area within the room, as the cooling effect would be intensified.

Therefore, the uneven distribution observed in the environment can be advantageous, allowing the cooling intensity to be adjusted according to the duration and severity of the heat event. In the early stages of a heatwave, when there is a sudden temperature rise, directing the EC toward occupants intensifies and accelerates the cooling effect. However, prolonged exposure to high air speed can cause eye dryness and discomfort in sensitive tissues. Therefore, after initial relief, the EC can be redirected towards a wall to provide indirect and distributed air flow. To maximize the effect, local ECs should be used by occupants, which provides a smoother air flow and allows personal adjustment to individual preferences and needs. In addition, according to the mapping, people standing close to the wall toward which the EC outlet is directed will experience a more intense cooling effect than those standing farther away from that wall. Thus, positioning within the space can serve as a secondary strategy for personal adjustment. Indirect whole-room EC effect avoids local discomfort from direct high-speed air while delivering substantial heat loss over longer periods ($\geq$ 50 min), as demonstrated in this study's test conditions.

This strategy is particularly valuable for protecting vulnerable populations such as the elderly and individuals with chronic illnesses, who experience disproportionate impact from extreme heat events [94]. Even modest reductions in ambient temperature combined with increased air movement can shift conditions below critical heat stress thresholds, significantly reducing health risks [39].

4.4. Water and energy consumption

One key challenge of EC systems is water consumption. During the tests, the whole-room unit used a relatively large amount of water (see Fig. 9), averaging 2.6 L/h. When normalized by the volume of the test chamber (76 m^3), this corresponds to 0.034 L/h·m^3. Nevertheless, indoor relative humidity remained below 55%, well below typical design values [84], suggesting limited risk of mold growth or other high-humidity-related issues under the tested conditions.

These values exceed those reported in a previous EnergyPlus simulation study [60], where hourly water consumption ranged from 0.42 to 0.68 L/h (5.5 to 8.9 mL/h·m^3) according to the climatic scenario. That study included two building envelope types (a poorly insulated heavyweight structure and a well-insulated lightweight one) at an air change rate of 0.5 h^{-1}, and four 2021 heatwave events in Sacramento, Madrid, Riyadh, and Rome.

Three main factors explain this discrepancy. First, the experimental tests began in hot and dry conditions, which increased the water needed to raise indoor humidity towards equilibrium. Second, the simulations assumed steady-state conditions and thereby did not capture the initial humidification peak that occurs during startup. Third, the tested EC unit may have been oversized for chamber volume, which would increase water evaporation compared to a properly sized device.

These findings underscore that water should not be overlooked and that transient startup phases should be included in any water consumption assessment, particularly when systems activate during emergencies or short-duration heatwaves. Longer operating periods would likely lower the average water use once equilibrium is reached, but further research should confirm this through long-term tests under varying initial conditions and with different EC capacities. Water consumption should be further investigated as heatwaves are often associated with drought, limiting the availability of this resource.

EC systems also demonstrated a clear advantage in energy efficiency compared with traditional vapor-compression air-conditioning (AC). In this study, the whole-room EC operated at 220 W, and the personal EC at only 10 W; substantially lower than the power demand of typical AC units. A previous simulation study [60] found that evaporative coolers reduced daily electricity use by 62–74% compared to AC, while maintaining the same indoor setpoint temperature.

This substantial reduction in energy consumption highlights the potential of EC systems as an alternative cooling strategy, particularly for households without air-conditioning, and is especially relevant during heatwaves. Their minimal power requirements make ECs strong candidates for integration with battery storage, enabling continued operation during power outages or enabling users to shift consumption away from peak-demand periods. Battery-supported EC units could provide essential thermal relief in emergencies, particularly for

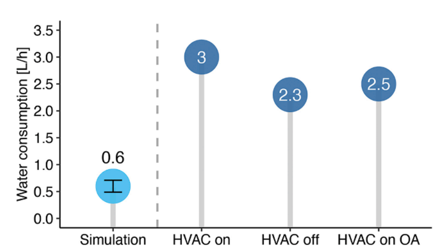

Fig. 9. Hourly water consumption of the evaporative cooler in the three experimental scenarios, compared with the average value obtained in a previous simulation study [60]. The error bar associated with the simulation category represents the standard deviation across all simulated scenarios, each of which assumed steady-state indoor conditions.

vulnerable populations without access to conventional air-conditioning.

4.5. Limitations and future work

A key limitation of this study is the use of a thermal manikin without sweating capability. This limitation likely leads to an underestimation of the actual cooling potential of evaporative systems, because evaporative heat loss from the skin plays a dominant role in total heat loss in warm weather conditions [39].

In addition, the whole-room EC produced relatively high uncertainty in its measured cooling effect, as indicated by the standard deviation in the power data (Fig. 4). This variability reflects the non-uniform impact of the EC on the manikin, driven by dynamic airflow distribution and environmental conditions. In contrast, the local EC showed lower variability (Fig. 7), resulting in more robust and consistent results. Future work should therefore include repeated trials, tests in a more controlled air flow environment (such as a wind tunnel or larger chamber), and experiments evaluating different equipment positions. Mapping the cooling effect at different points in the room can provide numerical references for the presented guidelines for equipment positioning applicable to other tested equipment as well.

Further research with human participants is crucial to validating these findings, incorporating physiological responses, subjective comfort perceptions, and user-experiment assessment. Such studies will provide critical data to refine EC designs, optimize operational strategies, and enhance their practical applicability during heat waves.

Moreover, the experiments were conducted under a single indoor starting condition (32 °C and low relative humidity), selected both as a representative hot-dry heatwave scenario and to ensure stable and repeatable operation of the climate chamber during transient measurements. These test conditions are the most favorable for enhancing the evaporative cooling effect. Therefore, future work should extend the analysis to a broader range of temperature and humidity conditions to better characterize the sensitivity and limits of evaporative cooling performance across different climatic scenarios.

Further experiments are also needed to characterize the short- and long-term water consumption of portable evaporative coolers under varying products, capacities, and environmental conditions, enabling the development of predictive models and comparisons with other types of ECs [95].

The experimental dataset, publicly available, may additionally serve as a benchmark for validating thermal simulations or CFD models incorporating EC systems, particularly for the calibration of convective heat transfer coefficients, humidity dynamics, and transient cooling behavior.

Finally, long-term field studies should investigate real-world operation patterns, occupant preferences, interactions with natural ventilation and intermittent use, and the influence of varying indoor environmental conditions during heatwaves.

5. Conclusions

This study experimentally demonstrates the effectiveness of evaporative coolers (ECs) in improving indoor thermal conditions during hot and dry heatwave scenarios. Whole-room ECs reduced air temperature by up to 2.8 K, while the dry-losses cooling effect (CE) on a thermal manikin reached 3 K and increased to 6 K when combined with a personal EC. These findings highlight that perceived thermal relief depends not only on air temperature and relative humidity but also on airflow dynamics.

Airflow fluctuations appeared to enhance convective heat transfer, contributing to cooling even under modest air temperature reductions. Additionally, heterogeneous airflow patterns could be strategically leveraged to modulate cooling intensity according to the phase and duration of a heatwave. Directing airflow toward occupants offers rapid relief during short emergencies, whereas indirect circulation might be more suitable for prolonged exposures to avoid discomfort. Local EC can be added in both situations as it extends the effect with smoother and personally controllable air flow.

Energy demand remained low, 220 W for the whole-room EC and 10 W for the personal system, making these devices promising for heatwave refuges and resilient operation during power outages. The whole-room EC's power draw could be reduced further by selecting a unit appropriately sized for the room volume. However, whole-room water consumption averaged 2.6 L/h (equivalent to 0.034 L/h·m^3), exceeding previously simulation-based estimates under steady-state conditions of approximately 0.42–0.68 L/h (5.5–8.9 mL/h·m^3). This discrepancy reinforces the need to account for start-up transients, initial environmental dryness, and adequately sizing EC for real-world applications.

Overall, evaporative cooling provides a low-energy, fast-acting option for reducing heat strain during extreme heat events. The combined whole-room and personal cooling effects observed in this study show that EC systems can meaningfully increase heat loss and improve indoor thermal conditions, even when air-temperature reductions are modest. These results reinforce the value of evaporative cooling as a practical strategy for creating safer indoor environments during heatwaves, characterized by hot and dry conditions, particularly when rapid relief and low energy demand are essential.

Declaration of generative AI in the writing process

During the preparation of this work, we used Grammarly, Copilot and chatGPT to improve the readability and language of the manuscript, and to individually generate the icons included in the graphical abstract. All content was reviewed, edited, and approved. We take full responsibility for the final version of the publication.

CRediT authorship contribution statement

Roberto Rugani: Conceptualization, Data curation, Formal analysis, Investigation, Methodology, Software, Validation, Visualization, Writing – original draft, Writing – review & editing. **Maíra André:** Conceptualization, Data curation, Formal analysis, Investigation, Methodology, Software, Validation, Visualization, Writing – original draft, Writing – review & editing. **Marco Picco:** Conceptualization, Investigation, Supervision, Validation, Visualization, Writing – review & editing. **Giacomo Salvadori:** Conceptualization, Resources, Supervision, Visualization, Writing – review & editing. **Stefano Schiavon:** Methodology, Project administration, Resources, Supervision, Validation, Visualization, Writing – review & editing. **Roberto Lamberts:** Conceptualization, Resources, Supervision, Visualization, Writing – review & editing. **Hui Zhang:** Conceptualization, Funding acquisition, Methodology, Project administration, Resources, Supervision, Validation, Visualization, Writing – review & editing.

Declaration of competing interest

The authors declare that they have no known competing financial interests or personal relationships that could have appeared to influence the work reported in this paper.

Acknowledgement

Maíra André would like to acknowledge the financial support received by Coordination for the Improvement of Higher Education Personnel (CAPES). Roberto Rugani would like to acknowledge the financial support received by the University of Pisa for doctoral student mobility.

We gratefully acknowledge Big Ass Fans for providing the whole-room evaporative cooler used in this study.

Appendix A. Local EC mapping

The higher cooling effect is expected to be associated with higher air speed and lower air temperature produced by the local EC. Fig. 10 shows a linear mapping produced by 4 probes positioned between the local EC and the manikin to capture air temperature and air speed from the EC outlet to the manikin. The greatest temperature reduction occurred at the outlet, while the highest velocity occurred between the outlet and the manikin's chest. The outlet air temperature was similar at both activation levels (low and high), averaging around 24 °C. However, under the high-speed setting, the air temperature at chest level was 0.4 K lower than the room temperature, whereas under the low-speed setting, it remained unchanged at approximately 28 °C. The difference in air speed between activation levels is much greater, achieving a maximum of 3.3 m/s at low and 4.7 m/s at high settings, more than 1 m/s of difference. The velocity reaching the manikin's torso is significantly lower with a smaller difference, 0.2 m/s and 0.5 m/s at low and high levels, respectively. The difference between the two activation levels at the maximum point and the manikin chest explains the difference in the cooling effect across the body. The mid position, where a higher air speed is verified, also matches a lower temperature than the chest, around 25.4–25.8 °C. These values are closer to the conditions achieved at the upper and lower arms, which are closer to the local EC. This matches the higher cooling effect observed on those body parts (see Fig. 8). Although the air speed is lower and air temperature higher on the chest, this body part accounts for a greater area, resulting in a larger impact on the total cooling effect indicated in Fig. 7.

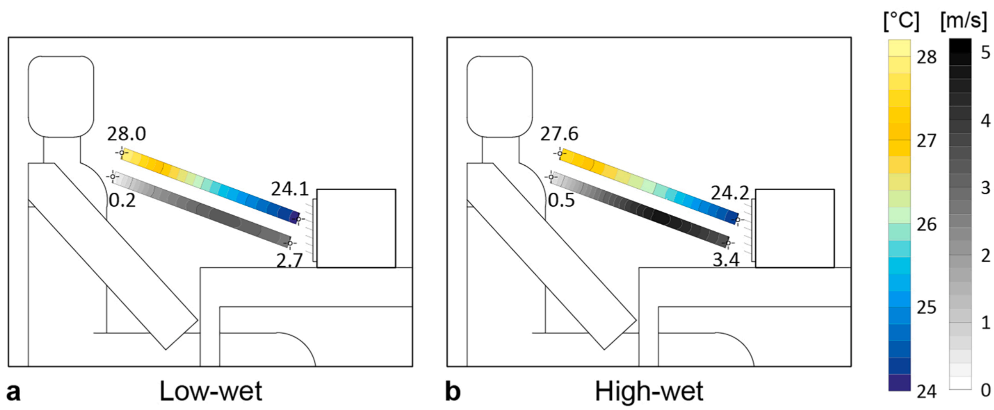

Fig. 10. Linear distribution of air temperature (color scale) and air speed (grey scale) for a) low and b) high EC speed levels with wet pad. Labels indicate values at the EC outlet of the manikin chest. The horizontal distance between those points is 50 cm.

Data availability

The data supporting the findings of this study, together with the code used for data processing and analysis, are publicly available on GitHub at https://github.com/mairaUSYD/EvaporativeCool.git.

References

[1] IPCC, Climate Change 2022: Impacts, Adaptation and Vulnerability, Cambridge University Press, Cambridge, UK and New York, USA, 2022.
[2] F.S. Kanti, A. Alari, B. Chaix, T. Benmarhnia, Comparison of various heat waves definitions and the burden of heat-related mortality in France: implications for existing early warning systems, Environ. Res. 215 (2022) 114359, https://doi.org/10.1016/j.envres.2022.114359.
[3] World Health Organization (WHO), World Meteorological Organization (WMO), Heatwaves and Health: Guidance On Warning-System Development, World Health Organization, Geneva, 2015. https://www.who.int/publications/m/item/heatwaves-and-health-guidance-on-warning-system-development (accessed June 25, 2025).
[4] J. Vanos, G. Guzman-Echavarria, J.W. Baldwin, C. Bongers, K.L. Ebi, O. Jay, A physiological approach for assessing human survivability and liveability to heat in a changing climate, Nat. Commun. 14 (2023) 7653, https://doi.org/10.1038/s41467-023-43121-5.
[5] World Health Organization (WHO), Heat and health. https://www.who.int/news-room/fact-sheets/detail/climate-change-heat-and-health, 2024 (accessed June 25, 2025).
[6] N.S. Bedi, Q.H. Adams, J.J. Hess, G.A. Wellenius, The role of cooling centers in protecting vulnerable individuals from extreme heat, Epidemiology (Fairfax) 33 (2022) 611–615, https://doi.org/10.1097/EDE.0000000000001503.
[7] C. Dearman, N. Adams, K. Brooks, A. Sousa, N. Pearce-Smith, C. Petrokofsky, Public health effectiveness of cooling centres during periods of adverse hot weather: a systematic literature review, Oxford Open Clim. Change 5 (2025), https://doi.org/10.1093/oxfclm/kgaf020.
[8] A.T. Amorim-Maia, I. Anguelovski, J. Connolly, E. Chu, Seeking refuge? The potential of urban climate shelters to address intersecting vulnerabilities, Landsc. Urban Plan. 238 (2023) 104836, https://doi.org/10.1016/j.landurbplan.2023.104836.
[9] S.G. Nayak, S. Shrestha, S.C. Sheridan, W.-H. Hsu, N.A. Muscatiello, C.I. Pantea, Z. Ross, P.L. Kinney, M. Zdeb, S.-A.A. Hwang, S. Lin, Accessibility of cooling centers to heat-vulnerable populations in New York State, J. Transp. Health 14 (2019) 100563, https://doi.org/10.1016/j.jth.2019.05.002.
[10] R.D. Meade, S.R. Notley, A.P. Akerman, J.J. McCormick, K.E. King, R.J. Sigal, G. P. Kenny, Efficacy of cooling centers for mitigating physiological strain in older adults during daylong heat exposure: a laboratory-based heat wave simulation, Environ. Health Perspect. 131 (2023), https://doi.org/10.1289/EHP11651.
[11] S. Roaf, Architecture for a different future. Living With Climate Change, Elsevier, 2024, pp. 67–88, https://doi.org/10.1016/B978-0-443-18515-1.00014-9.
[12] S. Chen, L. Zhao, Q. Li, J. Yang, S. Zhang, Z. Nie, A. Wagner, Linking outdoor heatwave and indoor overheating: a multi- timescale coupling framework for residential buildings in hot and humid climates, Build. Environ. 289 (2026) 114086, https://doi.org/10.1016/j.buildenv.2025.114086.
[13] L. Davis, P. Gertler, S. Jarvis, C. Wolfram, Air conditioning and global inequality, Glob. Environ. Change 69 (2021) 102299, https://doi.org/10.1016/j.gloenvcha.2021.102299.
[14] G. Falchetta, E. De Cian, F. Pavanello, I.S. Wing, Inequalities in global residential cooling energy use to 2050, Nat. Commun. 15 (2024) 7874, https://doi.org/10.1038/s41467-024-52028-8.
[15] United Nations Environment Programme, Global cooling watch 2025: the free degrees, United Nations, 2025. 10.59117/20.500.11822/48926.
[16] S. Hajat, M. O'Connor, T. Kosatsky, Health effects of hot weather: from awareness of risk factors to effective health protection, Lancet 375 (2010) 856–863, https://doi.org/10.1016/S0140-6736(09)61711-6.
[17] H. Pallubinsky, R.P. Kramer, W.D. van Marken Lichtenbelt, Establishing resilience in times of climate change—a perspective on humans and buildings, Clim. Change 176 (2023) 135, https://doi.org/10.1007/s10584-023-03614-0.
[18] IEA, Staying cool without overheating the energy system, Paris, 2025.
[19] D.W. Abel, T. Holloway, M. Harkey, P. Meier, D. Ahl, V.S. Limaye, J. Patz, Air-quality-related health impacts from climate change and from adaptation of cooling demand for buildings in the eastern United States: an interdisciplinary modeling study, PLoS Med. 15 (2018) e1002599, https://doi.org/10.1371/journal.pmed.1002599.
[20] J. Woods, N. James, E. Kozubal, E. Bonnema, K. Brief, L. Voeller, J. Rivest, Humidity's impact on greenhouse gas emissions from air conditioning, Joule 6 (2022) 726–741, https://doi.org/10.1016/j.joule.2022.02.013.
[21] N. Shah, M. Wei, V. Letschert, A. Phadke, Benefits of Leapfrogging to Superefficiency and Low Global Warming Potential Refrigerants in Room Air

Conditioning, Lawrence Berkeley National Laboratory, 2015. https://escholarship.org/uc/item/584131r9 (accessed March 23, 2023).
[22] A. Malik, C. Bongers, B. McBain, O. Rey-Lescure, R. de Dear, A. Capon, M. Lenzen, O. Jay, The potential for indoor fans to change air conditioning use while maintaining human thermal comfort during hot weather: an analysis of energy demand and associated greenhouse gas emissions, Lancet Planet. Health 6 (2022) e301–e309, https://doi.org/10.1016/S2542-5196(22)00042-0.
[23] O. Jay, R. Hoelzl, J. Weets, N. Morris, T. English, L. Nybo, J. Niu, R. de Dear, A. Capon, Fanning as an alternative to air conditioning – a sustainable solution for reducing indoor occupational heat stress, Energy Build. 193 (2019) 92–98, https://doi.org/10.1016/j.enbuild.2019.03.037.
[24] T. Hoyt, E. Arens, H. Zhang, Extending air temperature setpoints: simulated energy savings and design considerations for new and retrofit buildings, Build. Environ. 88 (2015) 89–96, https://doi.org/10.1016/j.buildenv.2014.09.010.
[25] S. Schiavon, A.K. Melikov, Energy saving and improved comfort by increased air movement, Energy Build. 40 (2008) 1954–1960, https://doi.org/10.1016/j.enbuild.2008.05.001.
[26] A. Lipczynska, S. Schiavon, L.T. Graham, Thermal comfort and self-reported productivity in an office with ceiling fans in the tropics, Build. Environ. 135 (2018) 202–212, https://doi.org/10.1016/j.buildenv.2018.03.013.
[27] O. Jay, A. Capon, P. Berry, C. Broderick, R. de Dear, G. Havenith, Y. Honda, R. S. Kovats, W. Ma, A. Malik, N.B. Morris, L. Nybo, S.I. Seneviratne, J. Vanos, K. L. Ebi, Reducing the health effects of hot weather and heat extremes: from personal cooling strategies to green cities, Lancet 398 (2021) 709–724, https://doi.org/10.1016/S0140-6736(21)01209-5.
[28] W. Chen, H. Zhang, E. Arens, M. Luo, Z. Wang, L. Jin, J. Liu, F.S. Bauman, P. Raftery, Ceiling-fan-integrated air conditioning: airflow and temperature characteristics of a sidewall-supply jet interacting with a ceiling fan, Build. Environ. 171 (2020) 106660, https://doi.org/10.1016/j.buildenv.2020.106660.
[29] M.G. Kent, N.K. Huynh, A.K. Mishra, F. Tartarini, A. Lipczynska, J. Li, Z. Sultan, E. Goh, G. Karunagaran, A. Natarajan, A. Indrajith, I. Hendri, K.I. Narendra, V. Wu, N. Chin, C.P. Gao, M. Sapar, A. Seoh, N. Shuhadah, S. Valliappan, T. Jukes, C. Spanos, S. Schiavon, Energy savings and thermal comfort in a zero energy office building with fans in Singapore, Build. Environ. 243 (2023) 110674, https://doi.org/10.1016/j.buildenv.2023.110674.
[30] C. Koppe, S. Kovats, G. Jendritzky, B. Menne, D.J. Breuer, Heat Waves: Risks and Responses, Regional Office for Europe, World Health Organization, 2004.
[31] CDCUS, Frequently asked questions (FAQ) about extreme heat. https://www.cdc.gov/disasters/extremeheat/faq.html, 2012 (accessed March 23, 2023).
[32] R.D. Meade, S.R. Notley, N.V Kirby, G.P. Kenny, A critical review of the effectiveness of electric fans as a personal cooling intervention in hot weather and heatwaves, Lancet Planet. Health 8 (2024) e256–e269, https://doi.org/10.1016/S2542-5196(24)00030-5.
[33] E. Mihalcin, S. Schiavon, N. Ravanelli, Examining the physiological strain with electric fans during high indoor heat stress, Build. Environ. 282 (2025) 113261, https://doi.org/10.1016/j.buildenv.2025.113261.
[34] O. Jay, M.N. Cramer, N.M. Ravanelli, S.G. Hodder, Should electric fans be used during a heat wave? Appl. Ergon. 46 (2015) 137–143, https://doi.org/10.1016/j.apergo.2014.07.013.
[35] N.B. Morris, T. English, L. Hospers, A. Capon, O. Jay, The effects of electric fan use under differing resting heat index conditions: a clinical trial, Ann. Intern. Med. 171 (2019) 675–677, https://doi.org/10.7326/M19-0512.
[36] N.M. Ravanelli, S.G. Hodder, G. Havenith, O. Jay, Heart rate and body temperature responses to extreme heat and humidity with and without electric fans, JAMA J. Am. Med. Assoc. 313 (2015) 724, https://doi.org/10.1001/jama.2015.153.
[37] D. Gagnon, S. Romero, M. Cramer, O. Jay, C. Crandall, Cardiac and thermal strain of elderly adults exposed to extreme heat and humidity with and without electric fan use, JAMA J. Am. Med. Assoc. 316 (2016) 989, https://doi.org/10.1001/jama.2016.10550.
[38] N.B. Morris, G.K. Chaseling, T. English, F. Gruss, M.F. Bin Maideen, A. Capon, O. Jay, Electric fan use for cooling during hot weather: a biophysical modelling study, Lancet Planet. Health 5 (2021) e368–e377, https://doi.org/10.1016/S2542-5196(21)00136-4.
[39] F. Tartarini, S. Schiavon, O. Jay, E. Arens, C. Huizenga, Application of Gagge's energy balance model to determine humidity-dependent temperature thresholds for healthy adults using electric fans during heatwaves, Build. Environ. 207 (2022) 108437, https://doi.org/10.1016/j.buildenv.2021.108437.
[40] A.P. Gagge, J.A.J. Stolwijk, Y. Nishi, An effective temperature scale based on a simple model of human physiological regulatory response, ASHRAE Trans. 77 (1971) 247–262.
[41] B.R. Hughes, H.N. Chaudhry, S.A. Ghani, A review of sustainable cooling technologies in buildings, Renew. Sustain. Energy Rev. 15 (2011) 3112–3120, https://doi.org/10.1016/j.rser.2011.03.032.
[42] Y. Yang, G. Cui, C.Q. Lan, Developments in evaporative cooling and enhanced evaporative cooling - a review, Renew. Sustain. Energy Rev. 113 (2019) 109230, https://doi.org/10.1016/j.rser.2019.06.037.
[43] H.T. El-Dessouky, H.M. Ettouney, W. Bouhamra, A novel air conditioning system: membrane air drying and evaporative cooling, Chem. Eng. Res. Des. 78 (2000) 999–1009, https://doi.org/10.1205/026387600528111.
[44] M. Jradi, S. Riffat, Experimental and numerical investigation of a dew-point cooling system for thermal comfort in buildings, Appl. Energy 132 (2014) 524–535, https://doi.org/10.1016/j.apenergy.2014.07.040.
[45] C. Farnham, K. Emura, T. Mizuno, Evaluation of cooling effects: outdoor water mist fan, Build. Res. Inf. 43 (2015) 334–345, https://doi.org/10.1080/09613218.2015.1004844.
[46] D. Abada, C. Maalouf, O. Sotehi, D. Rouag-Saffidine, G. Polidori, A.F. Boudjabi, Z. Derghout, Performance evaluation of fabrics for evaporative cooling applications, Energy Build. 266 (2022) 112120, https://doi.org/10.1016/j.enbuild.2022.112120.
[47] O. Amer, R. Boukhanouf, H.G. Ibrahim, A review of evaporative cooling technologies, Int. J. Environ. Sci. Dev. 6 (2015) 111–117, https://doi.org/10.7763/IJESD.2015.V6.571.
[48] N. Kapilan, A.M. Isloor, S. Karinka, A comprehensive review on evaporative cooling systems, Results Eng. 18 (2023) 101059, https://doi.org/10.1016/j.rineng.2023.101059.
[49] C. Yang, Z. Li, X. Cui, Q. Chen, X. Xiong, T. Wu, P. Yang, Numerical modelling and multifactor analysis of external tubes in a moisture-conducting fiber-assisted tubular indirect evaporative cooler, Int. J. Heat Mass Transf. 262 (2026) 128615, https://doi.org/10.1016/j.ijheatmasstransfer.2026.128615.
[50] L. Guan, M. Bennett, J. Bell, Evaluating the potential use of direct evaporative cooling in Australia, Energy Build. 108 (2015) 185–194, https://doi.org/10.1016/j.enbuild.2015.09.020.
[51] A. Al-Jubainawi, O.A.M. Mohammad, A.A.H. Al-Maidi, Z.A. Hussein, M. A. Abdelzaher, Sustainable thermal comfort assessment of evaporative cooling systems in hot and arid climates, Sci. Rep. 16 (2026) 14047, https://doi.org/10.1038/s41598-026-43175-7.
[52] A. Fouda, Z. Melikyan, A simplified model for analysis of heat and mass transfer in a direct evaporative cooler, Appl. Therm. Eng. 31 (2011) 932–936, https://doi.org/10.1016/j.applthermaleng.2010.11.016.
[53] D. Bishoyi, K. Sudhakar, Experimental performance of a direct evaporative cooler in composite climate of India, Energy Build. 153 (2017) 190–200, https://doi.org/10.1016/j.enbuild.2017.08.014.
[54] H. Hasani Balyani, A. Sohani, H. Sayyaadi, R. Karami, Acquiring the best cooling strategy based on thermal comfort and 3E analyses for small scale residential buildings at diverse climatic conditions, Int. J. Refrig. 57 (2015) 112–137, https://doi.org/10.1016/j.ijrefrig.2015.04.008.
[55] M.J. Romero-Lara, F. Comino, M. de Adana, Seasonal analysis comparison of three air-cooling systems in terms of thermal comfort, air quality and energy consumption for school buildings in Mediterranean climates, Energies (Basel) 14 (2021) 4436, https://doi.org/10.3390/en14154436.
[56] W. Chakroun, N. Ghaddar, K. Ghali, Chilled ceiling and displacement ventilation aided with personalized evaporative cooler, Energy Build. 43 (2011) 3250–3257, https://doi.org/10.1016/j.enbuild.2011.08.026.
[57] W. Shi, H. Yang, X. Ma, X. Liu, Techno-economic evaluation and environmental benefit of hybrid evaporative cooling system in hot-humid regions, Sustain. Cities Soc. 97 (2023) 104735, https://doi.org/10.1016/j.scs.2023.104735.
[58] S. Kashyap, J. Sarkar, A. Kumar, Performance assessment of dual-mode evaporative cooler for futuristic climatic scenarios considering climate change effect, J. Build. Eng. 42 (2021) 103043, https://doi.org/10.1016/j.jobe.2021.103043.
[59] S. Sudprasert, Utilization of an evaporative air cooler to achieve thermal comfort in Thailand, Build. Res. Inf. 49 (2021) 325–335, https://doi.org/10.1080/09613218.2020.1743962.
[60] R. Rugani, Y. Pan, H. Zhang, C. Huizenga, E. Arens, F. Fantozzi, M. Picco, Dynamic simulation of the effectiveness of evaporative cooling and fan in reducing heat strain during heatwaves, in: Proceedings of Building Simulation 2023: 18th Conference of IBPSA, IBPSA, Shanghai, CHN, 2023, https://doi.org/10.26868/25222708.2023.1685.
[61] R. Navon, H. Arkin, Feasibility of direct-indirect evaporative cooling for residences, based on studies with a desert cooler, Build. Environ. 29 (1994) 393–399, https://doi.org/10.1016/0360-1323(94)90040-X.
[62] ASHRAE, ANSI/ASHRAE standard 55-2023: "thermal environmental conditions for human occupancy," (2023).
[63] H. Zhang, E. Arens, Y. Zhai, A review of the corrective power of personal comfort systems in non-neutral ambient environments, Build. Environ. 91 (2015) 15–41, https://doi.org/10.1016/j.buildenv.2015.03.013.
[64] M. El Loubani, N. Ghaddar, K. Ghali, M. Itani, Hybrid cooling system integrating PCM-desiccant dehumidification and personal evaporative cooling for hot and humid climates, J. Build. Eng. 33 (2021) 101580, https://doi.org/10.1016/j.jobe.2020.101580.
[65] J.R. Camargo, C.D. Ebinuma, J.L. Silveira, Experimental performance of a direct evaporative cooler operating during summer in a Brazilian city, Int. J. Refrig. 28 (2005) 1124–1132, https://doi.org/10.1016/j.ijrefrig.2004.12.011.
[66] H. El-Dessouky, H. Ettouney, A. Al-Zeefari, Performance analysis of two-stage evaporative coolers, Chem. Eng. J. 102 (2004) 255–266, https://doi.org/10.1016/j.cej.2004.01.036.
[67] U. Sajjad, N. Abbas, K. Hamid, S. Abbas, I. Hussain, S.M. Ammar, M. Sultan, H. M. Ali, M. Hussain, Tauseef-ur-Rehman, C.C. Wang, A review of recent advances in indirect evaporative cooling technology, Int. Commun. Heat Mass Transf. 122 (2021) 105140, https://doi.org/10.1016/j.icheatmasstransfer.2021.105140.
[68] Y.M. Xuan, F. Xiao, X.F. Niu, X. Huang, S.W. Wang, Research and application of evaporative cooling in China: a review (I) – research, Renew. Sustain. Energy Rev. 16 (2012) 3535–3546, https://doi.org/10.1016/j.rser.2012.01.052.
[69] Z. Duan, C. Zhan, X. Zhang, M. Mustafa, X. Zhao, B. Alimohammadisagvand, A. Hasan, Indirect evaporative cooling: past, present and future potentials, Renew. Sustain. Energy Rev. 16 (2012) 6823–6850, https://doi.org/10.1016/j.rser.2012.07.007.
[70] H. Yang, W. Shi, Y. Chen, Y. Min, Research development of indirect evaporative cooling technology: an updated review, Renew. Sustain. Energy Rev. 145 (2021) 111082, https://doi.org/10.1016/j.rser.2021.111082.

[71] R. Caruana, S. De Antonellis, L. Marocco, M. Guilizzoni, Modeling of indirect evaporative cooling systems: a review, Fluids 8 (2023) 303, https://doi.org/10.3390/fluids8110303.
[72] P.M. Cuce, S. Riffat, A state of the art review of evaporative cooling systems for building applications, Renew. Sustain. Energy Rev. 54 (2016) 1240–1249, https://doi.org/10.1016/j.rser.2015.10.066.
[73] M.G. Haile, R. Garay-Martinez, A.M. Macarulla, Review of evaporative cooling systems for buildings in hot and dry climates, Buildings 14 (2024) 3504, https://doi.org/10.3390/buildings14113504.
[74] T.F. Ishugah, J. Kiplagat, J. Madete, J. Musango, Current status, challenges, and opportunities of evaporative cooling for building indoor thermal comfort using water as a refrigerant: a review, Int. J. Energy Res. 2024 (2024), https://doi.org/10.1155/2024/1026136.
[75] M. André, R. Rugani, H. Zhang, S. Schiavon, R. Lamberts, Boosting personal cooling with water: comparing a desk fan and evaporative coolers, in: Proceedings of the Comfort At The Extremes (CATE) Conference, Seville, 2024.
[76] M. André, C. Buonocore, L. De Castro, R. Lamberts, Users' assessment of personal fans in a warm office space in Brazil, J. Eng. Res. 18 (2021) 62–71, https://doi.org/10.53540/tjer.vol18iss2pp62-71.
[77] F. Bauman, E. Arens, The development of a controlled environment chamber for the physical and subjective assessment of human comfort in office environments, UC Berkeley: Center for the Built Environment (1988). https://escholarship.org/uc/item/0mn5485n.
[78] M. André, S. Schiavon, R. Lamberts, Implementation of desk fans in open office: lessons learned and guidelines from a field study, Build. Environ. 259 (2024) 111681, https://doi.org/10.1016/j.buildenv.2024.111681.
[79] T. Rinker, D. Kurkiewicz, K. Hughitt, A. Wang, G. Aden-Buie, L. Burk, pacman: package management tool, CRAN (2019).
[80] K. Müller, J. Bryan, here: a simpler way to find your files, CRAN (2020).
[81] V. Spinu, G. Grolemund, H. Wickham, D. Vaughan, I. Lyttle, I. Costigan, J. Law, D. Mitarotonda, J. Larmarange, J. Boiser, C.H. Lee, lubridate: make dealing with dates a little easier, CRAN (2024).
[82] S. Tanabe, E.A. Arens, H. Zhang, T. Madsen, Evaluating Thermal Environments By Using a Thermal Manikin With Controlled Skin Surface Temperature, UC Berkeley: Center for the Built Environment, 1994.
[83] S. Schiavon, A.K. Melikov, Introduction of a cooling-fan efficiency index, HVAC&R. Res. 15 (2009) 1121–1144, https://doi.org/10.1080/10789669.2009.10390882.
[84] ASHRAE, ANSI/ASHRAE standard 160-2021: "criteria for moisture-control design analysis In buildings", (2021).
[85] A.K. Mishra, M.G.L.C. Loomans, J.L.M. Hensen, Thermal comfort of heterogeneous and dynamic indoor conditions — an overview, Build. Environ. 109 (2016) 82–100, https://doi.org/10.1016/j.buildenv.2016.09.016.
[86] H. Zhang, E. Arens, C. Huizenga, T. Han, Thermal sensation and comfort models for non-uniform and transient environments, part III: whole-body sensation and comfort, Build. Environ. 45 (2010) 399–410, https://doi.org/10.1016/j.buildenv.2009.06.020.
[87] Y. Yu, J. Liu, K. Chauhan, R. de Dear, J. Niu, Experimental study on convective heat transfer coefficients for the human body exposed to turbulent wind conditions, Build. Environ. 169 (2020) 106533, https://doi.org/10.1016/j.buildenv.2019.106533.
[88] J.C.R. Hunt, E.C. Poulton, J.C. Mumford, The effects of wind on people; new criteria based on wind tunnel experiments, Build. Environ. 11 (1976) 15–28, https://doi.org/10.1016/0360-1323(76)90015-9.
[89] E. Mayer, Assessment of draught by an artificial skin, Build. Res. Pract. 5 (1989) 273–276.
[90] E. Mayer, New measurements of the convective heat transfer coefficient: influences of turbulence, mean air velocity and geometry of the human body, in: Roomvent '92, Third International Conference, Aalborg, Denmark, 1992.
[91] X. Xu, Y. Yu, H. Hong, G. Hu, J. Niu, Convective heat transfer coefficients over human body under non-uniform approaching airflow conditions, Energy Build. 339 (2025) 115778, https://doi.org/10.1016/j.enbuild.2025.115778.
[92] R. Caruana, L. Marocco, M. Guilizzoni, A novel CFD model for design and performance prediction of recuperators for indirect evaporative cooling, Therm. Sci. Eng. Prog. 51 (2024) 102619, https://doi.org/10.1016/j.tsep.2024.102619.
[93] D.J. Gibson, H.E. Kuder, S.B. Fey, What environmental features give rise to thermal refuges? A systematic review, Oikos n/a (n.d.) e11582. 10.1002/oik.11582.
[94] K.L. Ebi, A. Capon, P. Berry, C. Broderick, R. de Dear, G. Havenith, Y. Honda, R. S. Kovats, W. Ma, A. Malik, N.B. Morris, L. Nybo, S.I. Seneviratne, J. Vanos, O. Jay, Hot weather and heat extremes: health risks, Lancet 398 (2021) 698–708, https://doi.org/10.1016/S0140-6736(21)01208-3.
[95] C. Yang, Z. Li, S. Li, X. Cui, Q. Chen, Sustainable evaporative cooling driven by saline water sources: opportunities, challenges and solutions, Renew. Sustain. Energy Rev. 218 (2025) 115799, https://doi.org/10.1016/j.rser.2025.115799.